

# The motion of a point vortex around multiple circular islands

Darren G. Crowdy<sup>a)</sup> and Jonathan S. Marshall<sup>b)</sup>

*Department of Mathematics, Imperial College of Science, Technology and Medicine, 180 Queen's Gate, London SW7 2AZ, United Kingdom*

(Received 3 September 2004; accepted 3 March 2005; published online 5 May 2005)

A new constructive method for computing the motion of a single point vortex around an arbitrary finite number of circular islands in the special case when the circulations around all the islands are zero is presented. In this case, explicit representations for the governing Hamiltonians can be found and used to study the vortex trajectories. An example application is to geophysical flows and this study provides a simple model of the interaction of ocean eddies with topography. A wide range of illustrative examples are given, including the case of various multi-island configurations lying off an infinite coastline as well as in an unbounded ocean. The critical trajectories (or separatrices) dividing the flow domain into regions of qualitatively different dynamics of the vortices can be computed in a systematic and unified fashion irrespective of the number of islands present. © 2005 American Institute of Physics. [DOI: 10.1063/1.1900583]

## I. INTRODUCTION

The study of point vortex dynamics is an important area of fluid dynamics already commanding a vast literature. The review of Aref *et al.*<sup>1</sup> provides a recent survey of results involving vortex equilibria or “vortex crystals,” mainly in unbounded and periodic configurations, while the recent monograph of Newton<sup>2</sup> gives a broader perspective of the general  $N$ -vortex problem including discussions of vortex motion in unbounded and bounded planar domains as well as on curved surfaces such as the surface of a sphere.

While the motion of point vortices in unbounded domains has received much attention, much less developed is the theory of point vortex motion in domains bounded by impenetrable walls. The simplest example is a single point vortex adjacent to an infinite straight wall. Such a vortex translates at constant speed maintaining a constant distance from the wall. This motion is conveniently understood as being induced by an equal and opposite “image” vortex behind the wall. Another result in this area is the “Milne–Thomson circle theorem”<sup>3</sup> applying to the case of point vortices situated exterior to a circular cylinder. The famous solution known as the “Foppl vortex pair”<sup>2,4</sup> modeling the wake behind a cylinder in uniform flow is an example of a flow which can be derived using this general theorem.

A number of more elaborate examples involving simply connected fluid regions are given by Newton (Chapter 3),<sup>2</sup> others are described by Saffman.<sup>4</sup> Many of these examples rely on the transformation properties, under conformal mapping, of what is known as the Kirchhoff–Routh path function which is another designation of the Hamiltonian governing the vortex motion. The Hamiltonian formulation of point vortex dynamics, and the Kirchhoff–Routh path function, dates back to the work of Kirchhoff and Routh.<sup>5</sup> It was reappraised much later by Lin<sup>6,7</sup> who extended the Kirchhoff–

Routh approach to multiply connected domains, and more recently by Flucher and Gustafsson<sup>8</sup> who analyze various aspects of the general boundary value problem arising from point vortex motion in bounded domains.

The motion of a single vortex in bounded simply connected domains is relatively well studied. Flucher and Gustafsson<sup>8</sup> have shown that the Kirchhoff–Routh path function in this case satisfies an elliptic Liouville equation in the bounded domain and is infinite everywhere on its boundary. On the subject of  $N$ -vortex motion in multiply connected domains very little literature exists. Lin<sup>6</sup> establishes the existence and uniqueness of a generalized Kirchhoff–Routh path function in this case, but gives no explicit examples. In a recent paper, Johnson and McDonald<sup>9</sup> consider the motion of a vortex (which they model both as a point vortex and a vortex patch) in the doubly connected region exterior to two circular cylinders whose boundaries act as impenetrable barriers for the flow. The motivation for their study is to provide a simple model to understand how an oceanic eddy/vortex interacts with topography.<sup>10</sup> Such flow scenarios occur in a range of geophysical situations such as the interaction of Mediterranean salt lenses (Meddies) with seamounts in the Canary basin<sup>11</sup> or the collision of North Brazil Current rings with the islands of the Caribbean.<sup>12</sup> In their study, Johnson and McDonald<sup>9</sup> consider the case in which the circulation around each island is zero. By Kelvin’s circulation theorem, if this is true initially it will remain true at all subsequent times since all round-island circulations are conserved by the dynamics of the Euler equations. Other studies of geophysical interest involve the motion of vortices near gaps in an impenetrable barrier.<sup>13,14</sup> With oceanographic applications in mind, the case of point vortex motion, involving boundaries, on the surface of a sphere has also received attention.<sup>15</sup>

The present study generalizes the work of Johnson and McDonald<sup>9</sup> to the case of an essentially arbitrary finite number of circular islands (or cylinders). The treatment exploits some recent new mathematical results developed in Crowdy and Marshall.<sup>16</sup> There, explicit analytical formulas for the

<sup>a)</sup> Author to whom correspondence should be addressed. Electronic mail: d.crowdy@imperial.ac.uk

<sup>b)</sup> Electronic mail: jonathan.marshall@imperial.ac.uk

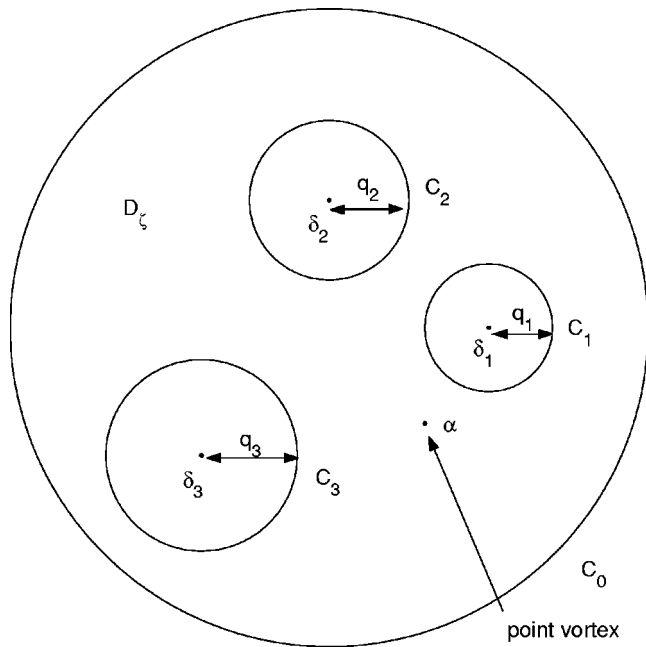


FIG. 1. Schematic of typical multiply connected circular region  $D_\zeta$ . The case shown, with three enclosed circles, is quadruply connected. There is a single point vortex at position  $\alpha(t)$ .  $C_0$  denotes the unit circle. There are  $M$  interior circles (the case  $M=3$  is shown here), each labeled  $\{C_j|j=1, \dots, M\}$ . The center of circle  $C_j$  is  $\delta_j$  and its radius is  $q_j$ .

Kirchhoff–Routh path functions for the  $N$ -vortex problem in circular domains of arbitrary finite connectivity are found in the special case in which all round-island circulations vanish. These formulas for the path function are reproduced here without proof, the interested reader being referred to Crowdy and Marshall<sup>16</sup> for full details of the mathematical derivation. While the derivation is involved, application of the final formula is relatively straightforward. It is one of the purposes of the present paper to highlight the efficacy of the formula, and its ease of application in modeling practical situations of geophysical interest, without obfuscating the presentation with the underlying mathematical proofs.

**II. MATHEMATICAL FORMULATION**

Let  $D_\zeta$  be a bounded circular domain with the outer boundary given by  $|\zeta|=1$ . Let  $M$  be a non-negative integer and let the boundaries of  $M$  enclosed circular disks be denoted  $\{C_j|j=1, \dots, M\}$ .  $M=0$  corresponds to the simply connected case where there are no enclosed circular disks. Let the radius of circle  $C_j$  be  $q_j \in \mathbb{R}$  and let its center be at  $\zeta = \delta_j \in \mathbb{C}$ . Such a domain is  $(M+1)$  connected. An example of a quadruply connected domain is shown in Fig. 1.

Let  $W(\zeta, \alpha)$  be the complex potential associated with an incompressible flow in  $D_\zeta$  which is irrotational except for a single point vortex singularity at  $\zeta=\alpha$ . The point vortex will be taken to have unit circulation while all the circulations around the  $M$  enclosed islands will be taken to be zero.  $W(\zeta, \alpha)$  must be analytic, but not necessarily single valued, everywhere in  $D_\zeta$  except for a logarithmic singularity at  $\zeta = \alpha$  corresponding to the point vortex. It must also be such that

$$\text{Im}[W(\zeta, \alpha)] = 0 \quad \text{on } |\zeta| = 1 \tag{1}$$

and

$$\text{Im}[W(\zeta, \alpha)] = \beta_j(t) \quad \text{on } C_j, \quad j = 1, \dots, M, \tag{2}$$

where the parameters  $\{\beta_j(t)\}$  depend possibly on time but not space. Conditions (1) and (2) ensure that all boundaries are streamlines. The choice (1) provides a normalization which uniquely determines  $W(\zeta, \alpha)$ . The values of  $\{\beta_j(t)|j=1, \dots, M\}$  are dictated by the zero-circulation conditions around the islands. Flucher and Gustafsson<sup>8</sup> give a comprehensive discussion of the mathematical problem of point vortex motion in multiply connected domains.

Crowdy and Marshall<sup>16</sup> show that an explicit formula for the complex potential  $W(\zeta, \alpha)$  satisfying all the conditions above is

$$W(\zeta, \alpha) = -\frac{i}{4\pi} \ln \left( \frac{\omega(\zeta, \alpha) \bar{\omega}(\zeta^{-1}, \alpha^{-1})}{\omega(\zeta, \bar{\alpha}^{-1}) \bar{\omega}(\zeta^{-1}, \bar{\alpha})} \right), \tag{3}$$

where  $\omega$  and  $\bar{\omega}$  are two special functions to be defined below. Let  $\psi$  be the streamfunction associated with the incompressible flow. Then

$$\psi = \text{Im}[W(\zeta, \alpha)]. \tag{4}$$

Formula (3) is the key result from Ref. 16 to be employed in what follows.

The functions  $\omega(\zeta, \alpha)$  and  $\bar{\omega}(\zeta, \alpha)$  are defined as follows. For each interior circle  $\{C_j|j=1, \dots, M\}$  of the domain  $D_\zeta$  (see Fig. 1), define the conformal map

$$\theta_j(\zeta) = \frac{a_j \zeta + b_j}{c_j \zeta + d_j}, \quad j = 1, \dots, M, \tag{5}$$

where

$$a_j = q_j - \frac{|\delta_j|^2}{q_j}, \quad b_j = \frac{\delta_j}{q_j}, \quad c_j = -\frac{\bar{\delta}_j}{q_j}, \quad d_j = \frac{1}{q_j}. \tag{6}$$

Conformal maps of the linear-fractional form (5) are known as *Möbius maps*.<sup>17</sup> With the  $M$  basic Möbius maps (5) together with their  $M$  inverses  $\{\theta_j^{-1}|j=1, \dots, M\}$  (which are also easily shown to be Möbius maps), an infinite number of additional Möbius maps can be generated by composition of these  $2M$  basic maps (it is easy to verify that the composition of two Möbius maps is another Möbius map). The infinite set of maps constructed in this way can be categorized according to their *level*. The *level one* maps will be the  $2M$  maps

$$\theta_1, \theta_2, \dots, \theta_M, \theta_1^{-1}, \theta_2^{-1}, \dots, \theta_M^{-1}, \tag{7}$$

the *level two* maps will be all compositions of any two of the above level one maps that do not reduce to a lower level map (i.e., the identity). Some level two maps include

$$\theta_1^2, \theta_1 \theta_2, \theta_1 \theta_2^{-1}, \dots, \theta_{M-1} \theta_M, \theta_M^2. \tag{8}$$

The *level three* maps are all those compositions of any three of the basic maps which do not reduce to a lower-level map. All higher level maps are defined similarly.

We define the conjugate maps  $\bar{\theta}_j(\zeta)$  to be

$$\overline{\theta_j(\zeta)} = \overline{\theta_j(\bar{\zeta})} \quad (9)$$

so that

$$\overline{\theta_j(\zeta)} = \frac{\bar{a}_j \bar{\zeta} + \bar{b}_j}{\bar{c}_j \bar{\zeta} + \bar{d}_j}, \quad j = 1, \dots, M. \quad (10)$$

Again, a second infinite set of Möbius maps can be generated by compositions of the  $2M$  basic maps  $\{\theta_j, \theta_j^{-1} | j=1, \dots, M\}$ . Given these two infinite sets of Möbius maps, the function  $\omega(\zeta, \gamma)$  is defined to be

$$\omega(\zeta, \gamma) = (\zeta - \gamma) \omega'(\zeta, \gamma), \quad (11)$$

where

$$\omega'(\zeta, \gamma) = \prod_{\theta_k} \frac{[\theta_k(\zeta) - \gamma][\theta_k(\gamma) - \zeta]}{[\theta_k(\zeta) - \zeta][\theta_k(\gamma) - \gamma]}, \quad (12)$$

and where the product is over all compositions of the basic maps  $\{\theta_j, \theta_j^{-1} | j=1, \dots, M\}$  excluding the identity map and all inverse maps. This means, for example, that if it is decided to include the level two map  $\theta_1[\theta_2(\zeta)]$ , then the map  $\theta_2^{-1}[\theta_1^{-1}(\zeta)]$  must *not* be included. Note that the prime notation is not used in this paper to denote derivatives.

The function  $\bar{\omega}(\zeta, \alpha)$  is defined similarly to be

$$\bar{\omega}(\zeta, \gamma) = (\zeta - \gamma) \bar{\omega}'(\zeta, \gamma), \quad (13)$$

where

$$\bar{\omega}'(\zeta, \gamma) = \prod_{\bar{\theta}_k} \frac{[\bar{\theta}_k(\zeta) - \gamma][\bar{\theta}_k(\gamma) - \zeta]}{[\bar{\theta}_k(\zeta) - \zeta][\bar{\theta}_k(\gamma) - \gamma]}, \quad (14)$$

and where the product is over all compositions of the basic maps  $\{\bar{\theta}_j, \bar{\theta}_j^{-1} | j=1, \dots, M\}$ , again excluding the identity map and all inverse maps.

In writing a numerical subroutine to compute the above functions, it is necessary to truncate the infinite products defining them. This can be done in a natural way by including all Möbius maps up to some level (as defined earlier). All the examples in this paper are computed by truncating the infinite products at level four, keeping all maps up to level three in the product. The truncation was checked by reevaluating various quantities by truncating at a higher level to make sure that convergence was reached.

We remark that while we have omitted any formal mathematical proofs that  $W(\zeta, \alpha)$  as given in (3) satisfies the boundary conditions listed earlier (the proofs are in Ref. 16), the interested reader can nevertheless verify this numerically, for a chosen  $D_\zeta$ , now that the functions  $\omega$  and  $\bar{\omega}$  have been defined. A further check on the validity of (3) appears later when we retrieve known results for the simply and doubly connected scenarios from our more general formulas (see Secs. III A and III B).

From (3) the associated streamfunction for the flow is given by the formula

$$\psi = \text{Im}[W(\zeta, \alpha)] = -\frac{1}{4\pi} \ln \left| \frac{\omega(\zeta, \alpha) \bar{\omega}(\zeta^{-1}, \alpha^{-1})}{\omega(\zeta, \bar{\alpha}^{-1}) \bar{\omega}(\zeta^{-1}, \bar{\alpha})} \right|. \quad (15)$$

Now let  $H^{(\zeta)}(\alpha, \bar{\alpha})$  denote the Hamiltonian (or Kirchoff–Routh path function) for the motion of the vortex in  $D_\zeta$ . The existence and uniqueness of such a function is established by Lin.<sup>6</sup> Following Lin<sup>6</sup> (see also Ref. 8) and on use of (15), a formula for  $H^{(\zeta)}(\alpha, \bar{\alpha})$  can be derived by decomposing the streamfunction as

$$\psi = -\frac{1}{2\pi} \ln |\zeta - \alpha| - \hat{\psi}(\zeta, \bar{\zeta}; \alpha, \bar{\alpha}), \quad (16)$$

where the function  $\hat{\psi}$  is regular at the point vortex singularity. The Hamiltonian for a point vortex of circulation  $\Gamma$  is then

$$H^{(\zeta)}(\alpha, \bar{\alpha}) = -\frac{\Gamma^2}{2} \hat{\psi}(\alpha, \bar{\alpha}; \alpha, \bar{\alpha}) \quad (17)$$

or, on use of (15) in (16),

$$H^{(\zeta)}(\alpha, \bar{\alpha}) = -\frac{\Gamma^2}{8\pi} \ln \left| \frac{1}{\alpha^2} \frac{\omega'(\alpha, \alpha) \bar{\omega}'(\alpha^{-1}, \alpha^{-1})}{\omega(\alpha, \bar{\alpha}^{-1}) \bar{\omega}(\alpha^{-1}, \bar{\alpha})} \right|. \quad (18)$$

This is an explicit formula for the Hamiltonian of a single vortex in the bounded circular domain  $D_\zeta$ . All the geometrical information on the shape of  $D_\zeta$  is neatly encoded in the functions  $\omega$  and  $\bar{\omega}$ . Referring back to the familiar “method of images”<sup>4</sup> mentioned in the Introduction, these special functions do all that is necessary to place an appropriate distribution of “image vortices” in the plane in such a way that all boundary conditions are simultaneously satisfied. In the multiply connected case, an infinite number of image vortices must be introduced and disposed in a complicated arrangement throughout the plane.

In order to find the Hamiltonian for motion in the more physically interesting case of vortex motion in *unbounded* circular domains, it is useful to employ a second result of Lin<sup>7</sup> showing how the Hamiltonian  $H^{(\zeta)}(\alpha, \bar{\alpha})$  transforms under arbitrary conformal mapping of the domain  $D_\zeta$ . Indeed, if  $D_\zeta$  maps to a domain  $D_z$  by means of a one-to-one conformal map  $z = z(\zeta)$ , then the Hamiltonian  $H^{(z)}$  in the image domain  $D_z$  is

$$H^{(z)}(z_\alpha, \bar{z}_\alpha) = H^{(\zeta)}(\alpha, \bar{\alpha}) + \frac{\Gamma^2}{4\pi} \ln |z_\zeta(\alpha)|, \quad (19)$$

where  $z_\alpha = z(\alpha)$ . Explicitly,

$$H^{(z)}(z_\alpha, \bar{z}_\alpha) = -\frac{\Gamma^2}{8\pi} \ln \left| \frac{1}{z_\zeta(\alpha)^2 \alpha^2} \frac{\omega'(\alpha, \alpha) \bar{\omega}'(\alpha^{-1}, \alpha^{-1})}{\omega(\alpha, \bar{\alpha}^{-1}) \bar{\omega}(\alpha^{-1}, \bar{\alpha})} \right|, \quad (20)$$

where it should be recalled that the one-to-one conformal mapping  $z = z(\zeta)$  is invertible so that, in principle,  $\zeta$  can be written as a function of  $z$ , i.e.,  $\zeta = \zeta(z)$ , or as is more relevant for the formula (20),  $\alpha = \alpha(z_\alpha)$ .

Finally, if there is an externally imposed background flow with associated complex potential  $W_B(z)$ , the Hamiltonian  $H_T^{(z)}(z_\alpha, \bar{z}_\alpha)$  of the total flow field becomes

$$H_T^{(z)}(z_\alpha, \bar{z}_\alpha) = H^{(z)}(z_\alpha, \bar{z}_\alpha) + H_B(z_\alpha, \bar{z}_\alpha), \tag{21}$$

where

$$H_B(z_\alpha, \bar{z}_\alpha) = \Gamma \operatorname{Im}[W_B(z_\alpha)]. \tag{22}$$

In this single degree-of-freedom Hamiltonian system in which  $H_T^{(z)}(z_\alpha, \bar{z}_\alpha)$  is conserved by the dynamics, the trajectories of the vortex are simply the contours of  $H_T^{(z)}(z_\alpha, \bar{z}_\alpha)$ .

### III. ISLANDS OFF A COASTLINE

The purpose of the next two sections is to demonstrate how readily the vortex trajectories around greatly differing island configurations can be found by exploiting the formulas above. The basic construction is the same irrespective of the number of islands present. This affords us a flexible and versatile means of constructing the vortex paths whatever the topology of the island configuration. All that changes from one example to the next is the set of preimage circles  $\{C_j | j = 1, \dots, M\}$  in the  $\zeta$  plane and therefore the functions  $\omega$  and  $\bar{\omega}$  appearing in the Hamiltonian.

First, consider the case in which a chain of islands exists off an infinite coastline. Let the imaginary axis in the  $z$  plane represent the coastline and consider a chain of  $M$  circular islands in the right half plane. This is the domain  $D_z$ . By the Riemann mapping theorem for multiply connected domains,<sup>18</sup> such a domain is conformally equivalent to *some* bounded circular domain  $D_\zeta$  of the type considered earlier.<sup>18</sup> Given a distribution of  $M$  islands in  $D_z$ , it remains to determine the geometrical arrangement of the  $M$  circles  $\{C_j | j = 1, \dots, M\}$  characterizing  $D_\zeta$ .

It is known<sup>17</sup> that Möbius maps take circles to circles, so to map  $D_\zeta$  to  $D_z$  we seek a Möbius map. Let  $|\zeta|=1$  map to the imaginary axis. If  $\zeta=1$  maps to  $z=0$  and  $\zeta=-1$  maps to infinity in the  $z$  plane, the relevant conformal mapping is

$$z(\zeta) = \frac{1 - \zeta}{1 + \zeta}. \tag{23}$$

The given centers and radii of the circles in the  $z$  plane dictate the values of the parameters  $\{q_j, \delta_j | j = 1, \dots, M\}$  in the preimage  $\zeta$  plane. Once the latter parameters are known, the functions  $\omega$  and  $\bar{\omega}$  can be constructed.

On use of (23) in both (18) and (19), the Hamiltonian in this case is

$$H^{(z)}(z_\alpha, \bar{z}_\alpha) = -\frac{\Gamma^2}{8\pi} \ln \left| \frac{(1 + \alpha)^4 \omega'(\alpha, \alpha) \bar{\omega}'(\alpha^{-1}, \alpha^{-1})}{4\alpha^2 \omega(\alpha, \alpha^{-1}) \bar{\omega}(\alpha^{-1}, \bar{\alpha})} \right|, \tag{24}$$

where  $z_\alpha = z(\alpha)$ .

Let  $Q_j$  be the radius and  $D_j$  the position of the center of the  $j$ th circle in the  $z$  plane. To determine  $\{q_j, \delta_j | j = 1, \dots, M\}$  from the specified parameters  $\{Q_j, D_j | j = 1, \dots, M\}$ , note that (23) is self-inverse so that

$$\zeta(z) = \frac{1 - z}{1 + z}. \tag{25}$$

Now, the equation for  $C_j$  is

$$\zeta \bar{\zeta} - \delta_j \bar{\zeta} - \bar{\delta}_j \zeta + |\delta_j|^2 - q_j^2 = 0. \tag{26}$$

Substituting (25) into (26) yields the following equation relating  $z, \bar{z}$ :

$$|z - D_j|^2 = Q_j^2, \tag{27}$$

where

$$D_j = \frac{1 - |\delta_j|^2 + q_j^2 + \bar{\delta}_j - \delta_j}{1 + |\delta_j|^2 - q_j^2 + \bar{\delta}_j + \delta_j} \tag{28}$$

and

$$Q_j = \frac{2q_j}{1 + |\delta_j|^2 - q_j^2 + \bar{\delta}_j + \delta_j}. \tag{29}$$

Two equations provided by (28) and (29) are to be solved for  $\{q_j, \delta_j | j = 1, \dots, M\}$  given the parameters  $\{Q_j, D_j | j = 1, \dots, M\}$ .

#### A. The simply connected case

It is instructive to see how our general approach for any finite connectivity reduces to the case of simply and doubly connected domains previously studied in the literature. This also provides an important check on the preceding analysis.

In the simply connected case, there are no enclosed circles to generate any Möbius maps so that

$$\omega'(\zeta, \gamma) = \bar{\omega}'(\zeta, \gamma) = 1, \tag{30}$$

$$\omega(\zeta, \gamma) = \bar{\omega}(\zeta, \gamma) = (\zeta - \gamma).$$

Substituting this into (24) yields

$$H^{(z)}(z_\alpha, \bar{z}_\alpha) = -\frac{\Gamma^2}{8\pi} \ln \left| \frac{(1 + \alpha)^4}{4} \frac{1}{(\alpha \bar{\alpha} - 1)^2} \right|. \tag{31}$$

But

$$z_\alpha = \frac{1 - \alpha}{1 + \alpha}, \quad \alpha = \frac{1 - z_\alpha}{1 + z_\alpha} \tag{32}$$

so that

$$\alpha \bar{\alpha} - 1 = -\frac{2(z_\alpha + \bar{z}_\alpha)}{(1 + z_\alpha)(1 + \bar{z}_\alpha)}, \tag{33}$$

$$1 + \alpha = \frac{2}{1 + z_\alpha}.$$

Substituting (33) into (31) yields

$$H^{(z)}(z_\alpha, \bar{z}_\alpha) = \frac{\Gamma^2}{4\pi} \ln |z_\alpha + \bar{z}_\alpha|, \tag{34}$$

which is well known (e.g., Ref. 2) to be the Hamiltonian for a single vortex near an infinite vertical wall.

**B. The doubly connected case**

A doubly connected domain can be obtained by a conformal mapping from some annulus  $q < |\zeta| < 1$  in a parametric  $\zeta$  plane. The value of  $q$  is determined by the domain itself. In this case,  $\delta_1 = 0$  and  $q_1 = q$ , so that the single Möbius map given by (5) is

$$\theta_1(\zeta) = q^2 \zeta. \tag{35}$$

Then,

$$\omega(\zeta, \gamma) = (\zeta - \gamma) \prod_{k=1}^{\infty} \frac{(q^{2k} \zeta - \gamma)(q^{2k} \gamma - \zeta)}{(q^{2k} \zeta - \zeta)(q^{2k} \gamma - \gamma)} = -\frac{\gamma}{C^2} P(\zeta/\gamma, q), \tag{36}$$

where

$$P(\zeta, q) \equiv (1 - \zeta) \prod_{k=1}^{\infty} (1 - q^{2k} \zeta)(1 - q^{2k} \zeta^{-1}) \tag{37}$$

and

$$C \equiv \prod_{k=1}^{\infty} (1 - q^{2k}). \tag{38}$$

Note also that since  $\bar{\theta}_1(\zeta) = \theta_1(\zeta)$  then  $\bar{\omega}(\zeta, \gamma) = \omega(\zeta, \gamma)$  in this case.

For a bounded doubly connected domain, the streamfunction becomes

$$\psi = -\frac{1}{4\pi} \ln \left| \frac{P(\zeta \alpha^{-1}, q) P(\alpha \zeta^{-1}, q)}{P(\zeta \bar{\alpha}, q) P(\zeta^{-1} \bar{\alpha}^{-1}, q)} \right|. \tag{39}$$

On use of the property that  $P(\zeta^{-1}, q) = -\zeta^{-1} P(\zeta, q)$  [which is easily established directly from the definition (37)], this reduces to

$$\psi = -\frac{1}{2\pi} \ln \left| \frac{\alpha P(\zeta \alpha^{-1}, q)}{P(\zeta \bar{\alpha}, q)} \right|. \tag{40}$$

$P(\zeta, q)$  is related to the first Jacobi theta function  $\Theta_1$ .<sup>19</sup> Indeed, defining

$$\tau = -\ln \zeta, \quad \tau_\alpha = -\ln \alpha \tag{41}$$

then the annulus in the  $\zeta$  plane is mapped to a rectangle in the  $\tau$  plane. It can be shown (see Ref. 19) that

$$P(\zeta, q) = -\frac{iC^{-1} e^{-\tau/2}}{q^{1/4}} \Theta_1[i\tau/2, q]. \tag{42}$$

On use of (42) it follows that

$$P(\zeta \alpha^{-1}, q) = -iC^{-1} q^{-1/4} \sqrt{\frac{\zeta}{\alpha}} \Theta_1[i(\tau - \tau_\alpha)/2, q], \tag{43}$$

$$P(\zeta \bar{\alpha}, q) = -iC^{-1} q^{-1/4} \sqrt{\zeta \bar{\alpha}} \Theta_1[i(\tau + \bar{\tau}_\alpha)/2, q],$$

which, on substitution into (40), yields

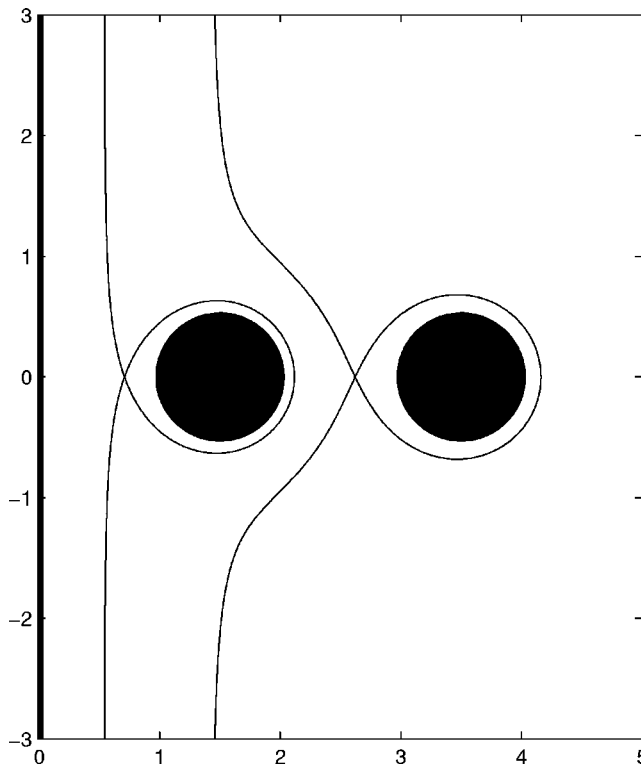


FIG. 2. Critical vortex trajectories for two islands of unit diameter off a coastline. The interisland separation  $d=1$ .

$$\psi = -\frac{1}{2\pi} \ln \left| \frac{\Theta_1[i(\tau - \tau_\alpha)/2, q]}{\Theta_1[i(\tau + \bar{\tau}_\alpha)/2, q]} \right|. \tag{44}$$

This is precisely the imaginary part of the complex potential given in Eq. (2.11) of Johnson and McDonald.<sup>9</sup>

**C. The higher-connected case**

Since the doubly connected case has been treated in detail in Ref. 9, no further examples are considered here. Instead, consider a triply connected fluid domain in which two circular islands are situated off an infinite coastline. Figure 2 shows the critical vortex trajectory for two islands, each of unit diameter, in horizontal alignment off a coastline. The first island is unit distance from the coast while the second island is separated by unit distance from the first. Figure 3 shows a more detailed distribution of trajectories. The critical vortex trajectories, or separatrices, can be found by identifying the position of the saddle points and finding the value of  $\psi$  associated with the contours passing through such points. This is done by using Newton's method to find the zeros of the derivative of the Hamiltonian at points on the real  $\zeta$  axis between the circles  $\{C_j\}$ . It follows from the symmetry in this case that the saddle points are on the real  $\zeta$  axis. No arrows are shown in the various figures of this paper but are determined by the sign of  $\Gamma$ . For example, if  $\Gamma > 0$ , the vortex travels down from  $y \rightarrow +\infty$ .

When the vortex is far from the two islands, it is expected that the vortex paths should become parallel to the coastline since the effect of the island cluster will be negligible and the vortex will see only its single image vortex in

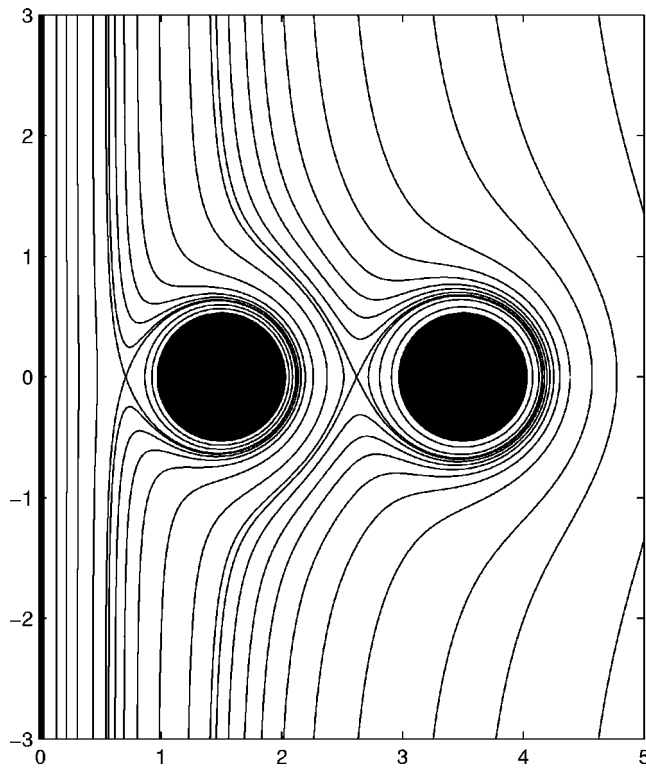


FIG. 3. Distribution of vortex trajectories around two unit-diameter islands off a coastline.

the straight coastline. As mentioned in the Introduction, the vortex will translate at constant speed maintaining a constant distance from the coastline. In terms of geophysical application, an interesting question is to ascertain how far from the coastline a distant approaching vortex must be in order to trace out qualitatively different paths as it approaches the island cluster. To perform such a study, consider two equal-sized islands of unit diameter in horizontal alignment in which one island is fixed to be unit distance from the coastline. Let  $d$ , an adjustable parameter, denote the horizontal separation of the two islands. Let  $d_1$  and  $d_2$  be the distances from the coastline of the two critical streamlines far away from the island cluster. Figure 4 shows a schematic. Using the above formulation, it is straightforward to systematically examine how  $d_1$  and  $d_2$  vary for differing interisland separations  $d$  (or indeed for any other geometrical parameter that one might choose to vary). Figure 5 shows the critical vortex trajectory for the four values  $d=0.5, 1.5, 2.5,$  and  $3.5$ . Figure 6 shows a graph of  $d_1$  and  $d_2$  against  $d$ . It is found that  $d_1$  remains almost constant as  $d$  is varied while  $d_2$  increases near-linearly with increasing  $d$ . This means that as the second island draws farther away from the coastline, vortices far upstream of the island cluster must also be farther away from the coastline in order to avoid traveling between the islands.

Additional islands can readily be incorporated into the approach. Figure 7 gives the critical vortex trajectory for three islands while Fig. 8 gives a more detailed path distribution in this case. These figures show three unit-diameter islands each separated from each other (in horizontal alignment) by unit distance, the leftmost island being unit distance from the coast. Even greater numbers of islands can be

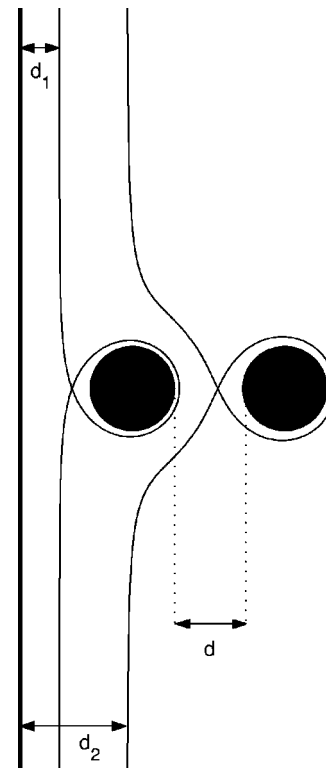


FIG. 4. Schematic for problem of two circular islands, separated by distance  $d$ , off a coastline. The two critical trajectories have far-field distances from the coast of  $d_1$  and  $d_2$ .

treated analogously without difficulty. Figures 9 and 10, respectively, show the critical vortex trajectories in the cases of four and five horizontally aligned islands. An interesting feature is that the area of vortex paths that encircle any given island gets larger for islands farther away from the coastline.

Other alignments of islands are also amenable to analysis. Figure 11 show vortex trajectories for the cases of two, three, and four islands in vertical alignment near a coastline. All islands have unit diameter and are separated from one another, and from the coastline, by unit distance. An interesting feature of these trajectories is that a vortex just to the left of the critical trajectory travels between the coastline and the island cluster with very little disturbance to what would be its path in the absence of the island cluster. However, vortices on paths just to the right of the critical trajectory diverge wildly from a straight vertical trajectory and, in passing to the right of each island, the vortex can be significantly drawn into each interisland region, getting very close to the coastline, and then moving back out again before being drawn back to the coastline in the region between the next two islands.

Besides horizontally and vertically aligned island clusters, staggered configurations are also of interest. Figures 12 and 13 show two and three islands, respectively, in various geometrical arrangements along the coastline. Note that the reflectional symmetry of the horizontally and vertically aligned configurations considered earlier are such that the circles in the  $\zeta$  plane are also reflectionally symmetric about the real  $\zeta$  axis so that  $\bar{\omega}(\zeta, \gamma) = \omega(\zeta, \gamma)$  and only one such function needs to be defined. However, the case shown in

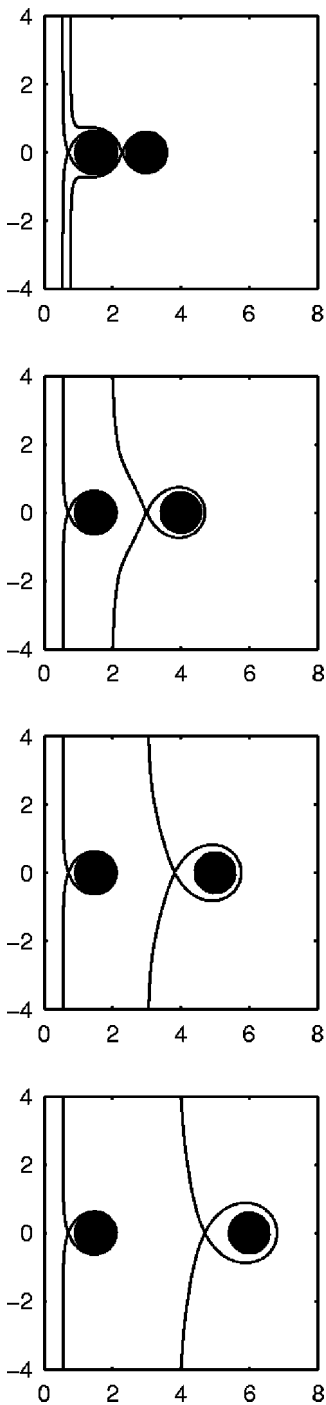


FIG. 5. Critical vortex trajectories for two unit-diameter islands at various separations  $d=0.5, 1.5, 2.5,$  and  $3.5$ .

Fig. 12 is an example in which  $\bar{\omega}(\zeta, \gamma) \neq \omega(\zeta, \gamma)$ , but the method encounters no additional difficulty. Figure 14 shows another example of trajectories around a randomly chosen three-island configuration with no geometrical symmetries at all.

**IV. ISLANDS IN UNBOUNDED OCEAN**

In the case of  $M+1$  islands in an unbounded ocean, each of the  $M$  enclosed circles  $\{C_j|j=1, \dots, M\}$  will be taken to map to the boundary of one of the islands. The circulation

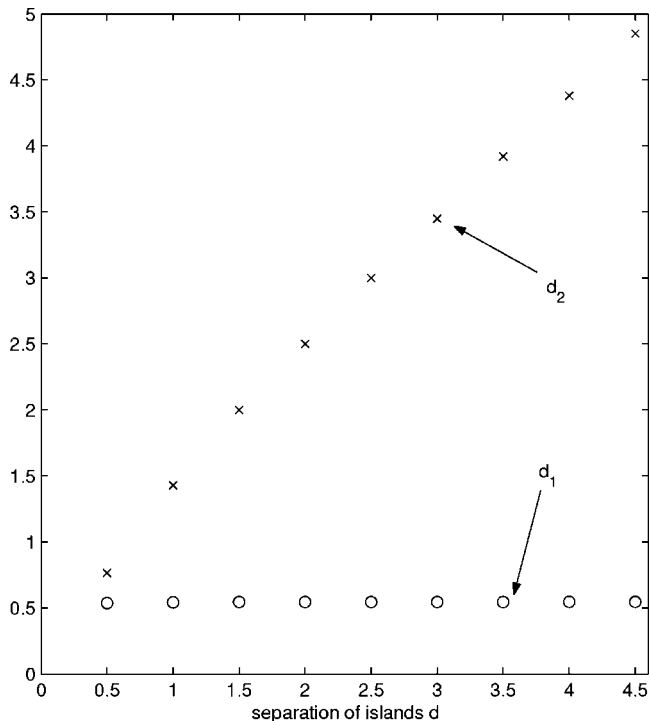


FIG. 6. Critical far-field distances away from coast— $d_1$  and  $d_2$ —as functions of the two-island separation  $d$ .

around these islands will be zero. The unit circle,  $|\zeta|=1$ , will be taken to map to the final island. In order that the image domain is unbounded, there must be a point denoted  $\zeta_\infty$  such that  $z(\zeta)$  has a simple pole at that point.

The circulation around the island corresponding to the image of  $|\zeta|=1$  will not, in general, be zero. In the calculations to follow, we choose to impose that the circulations around *all*  $M+1$  islands are zero. Such a situation arises, for example, when a vortex approaches the island cluster from far away, the initial flow around the islands being zero. To arrange this, it is necessary to add a point vortex of circula-

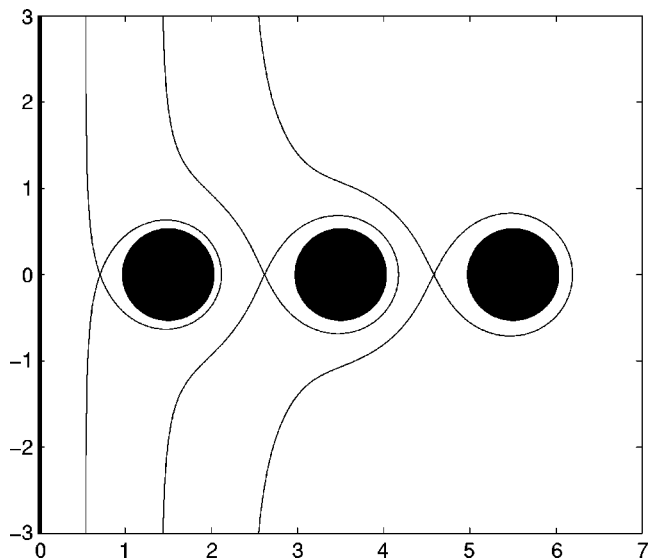


FIG. 7. Critical vortex trajectories for three unit-diameter islands separated by unit distance.

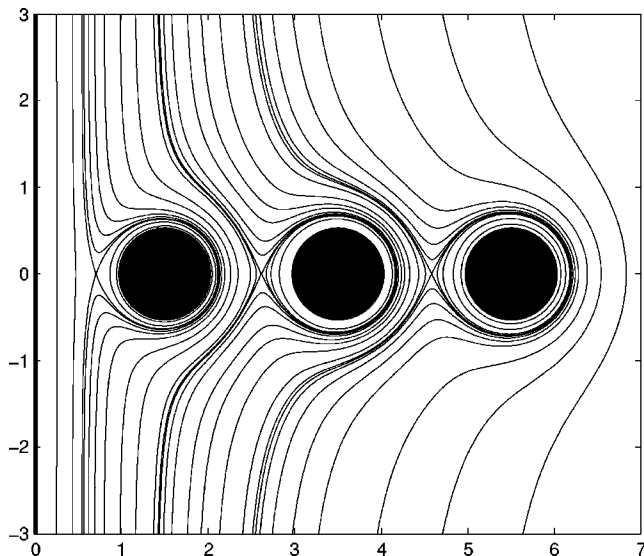


FIG. 8. Distribution of vortex trajectories for three unit-diameter islands off a coastline. The islands are separated by unit distance.

tion  $-\Gamma$  to the point at infinity in the  $z$  plane. Johnson and McDonald<sup>9</sup> employ a similar strategy in their study of the doubly connected case. The complex potential for the background flow associated with this point vortex at infinity is

$$W_B(\zeta) = \frac{i\Gamma}{4\pi} \ln \left( \frac{\omega(\zeta, \zeta_\infty) \bar{\omega}(\zeta^{-1}, \zeta_\infty^{-1})}{\omega(\zeta, \bar{\zeta}_\infty^{-1}) \bar{\omega}(\zeta^{-1}, \bar{\zeta}_\infty)} \right). \tag{45}$$

$$H^{(z)}(z_\alpha, \bar{z}_\alpha) = -\frac{\Gamma^2}{8\pi} \ln \left| \frac{1}{\alpha^2 |z_\zeta(\alpha)|^2} \frac{\omega'(\alpha, \alpha) \bar{\omega}'(\alpha^{-1}, \alpha^{-1}) \omega^2(\alpha, \bar{\zeta}_\infty^{-1}) \bar{\omega}^2(\alpha^{-1}, \bar{\zeta}_\infty)}{\omega(\alpha, \bar{\alpha}^{-1}) \bar{\omega}(\alpha^{-1}, \bar{\alpha}) \omega^2(\alpha, \zeta_\infty) \bar{\omega}^2(\alpha^{-1}, \zeta_\infty^{-1})} \right|, \tag{47}$$

where we have used (20) and (45) in (21) and (22).

The class of conformal maps to be used in the following examples is

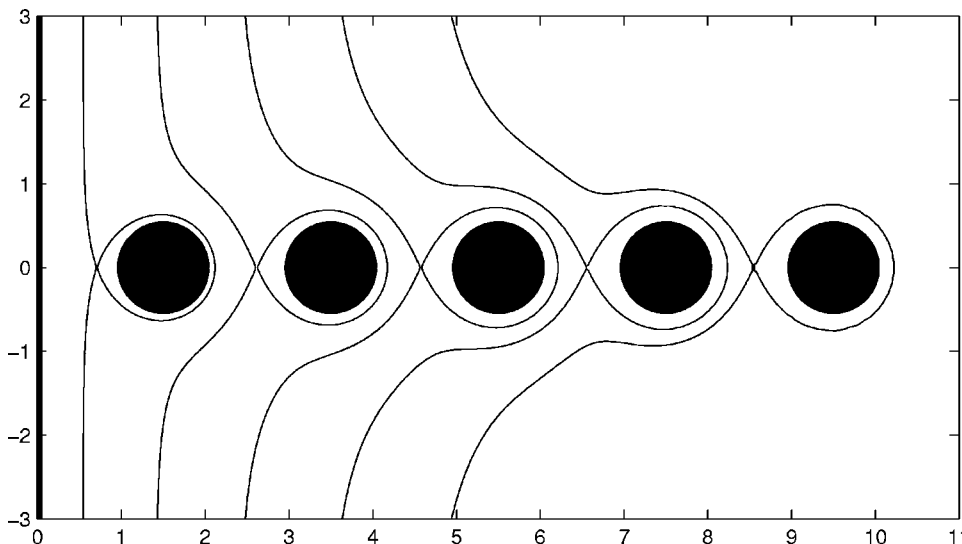


FIG. 10. Critical vortex trajectories for five unit-diameter islands off a coastline. The islands are separated by unit distance. The region of recirculation around the islands is greater for islands further from the coastline.

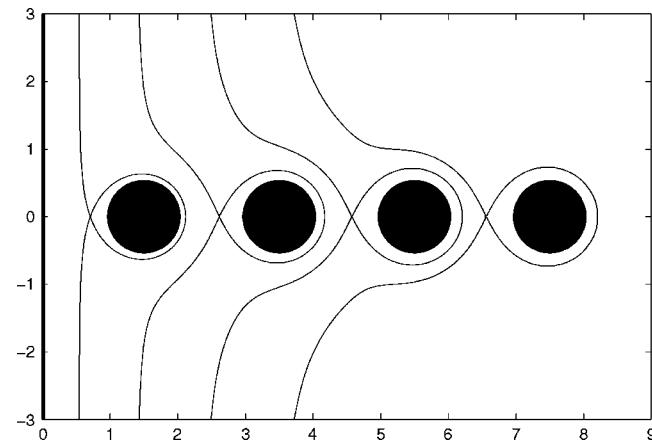


FIG. 9. Critical vortex trajectories for four unit-diameter islands off a coastline. The islands are separated by unit distance.

On a minor technical point, note that in the particular case when  $\zeta_\infty=0$  (which will in fact be the choice in the examples to follow) then the function  $\omega(\zeta, \infty)$  as given in (11) is not well defined. In this case, we instead use the modified formulas

$$\frac{\omega(\zeta, 0)}{\omega(\zeta, \infty)} = \zeta \frac{\omega'(\zeta, 0)}{\omega'(\zeta, \infty)}, \quad \frac{\bar{\omega}(\zeta, 0)}{\bar{\omega}(\zeta, \infty)} = \zeta \frac{\bar{\omega}'(\zeta, 0)}{\bar{\omega}'(\zeta, \infty)} \tag{46}$$

in (49) below. These are the appropriate generalizations since the functions on the right-hand sides of the two equations in (46) have a zero at  $\zeta=0$  and a pole at  $\zeta=\infty$ . The general form of the Hamiltonian in a conformally mapped  $z$  plane is then



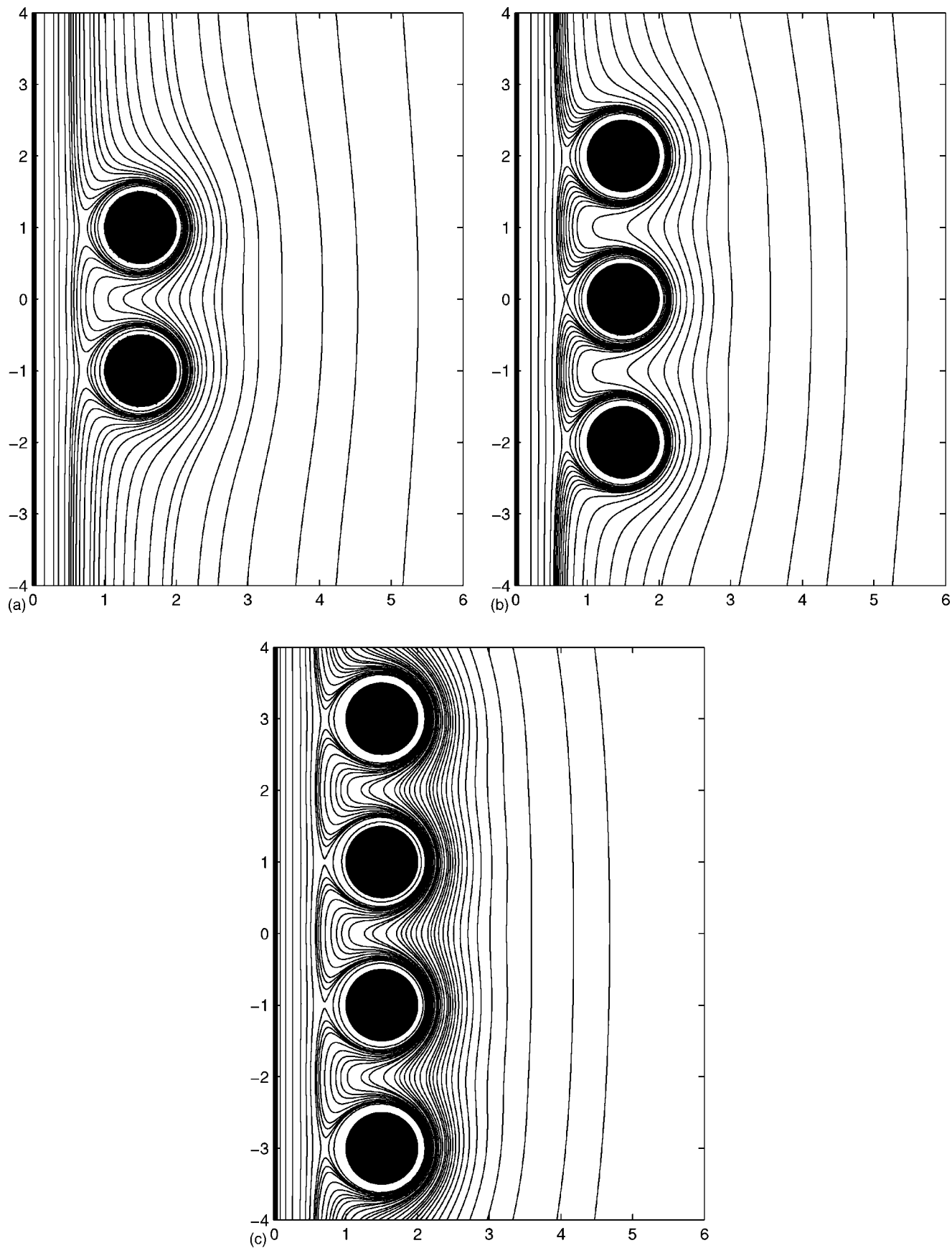


FIG. 11. Trajectories for two, three, and four unit-diameter islands aligned vertically at unit separation and at unit distance from a coastline. Vortices sufficiently close to the coastline travel close to the straight path they would take in the absence of the island cluster. Trajectories just to the right of the critical trajectory diverge wildly from this straight path.

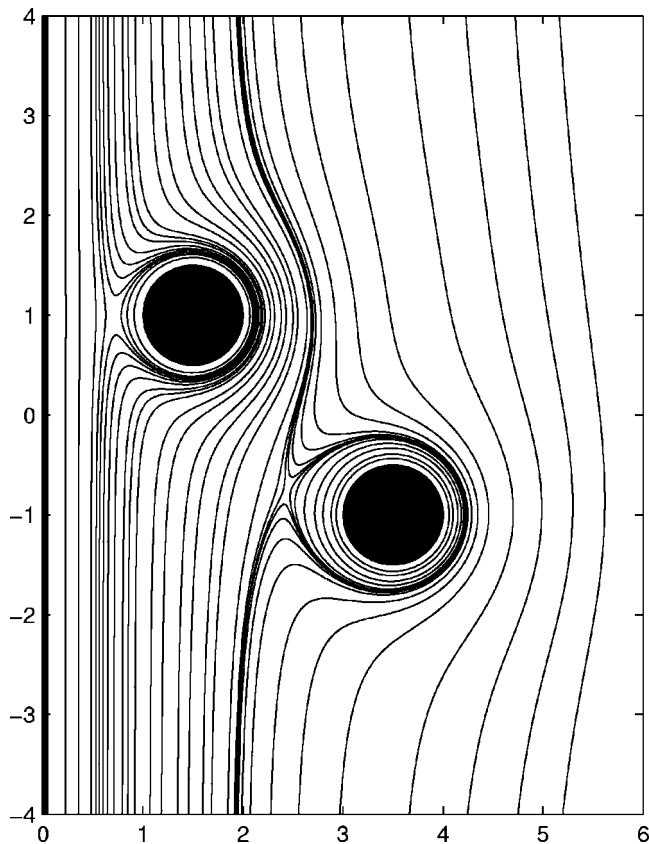


FIG. 12. Typical trajectories for two staggered islands near a coastline. Both have unit diameter, one is centered at  $1.5+i$  and the other at  $3.5-i$ .

$$z(\zeta) = \frac{a}{\zeta} + b, \tag{48}$$

where the real parameter  $a$  is chosen to fix the radius of the island corresponding to the image of  $|\zeta|=1$  and the (generally

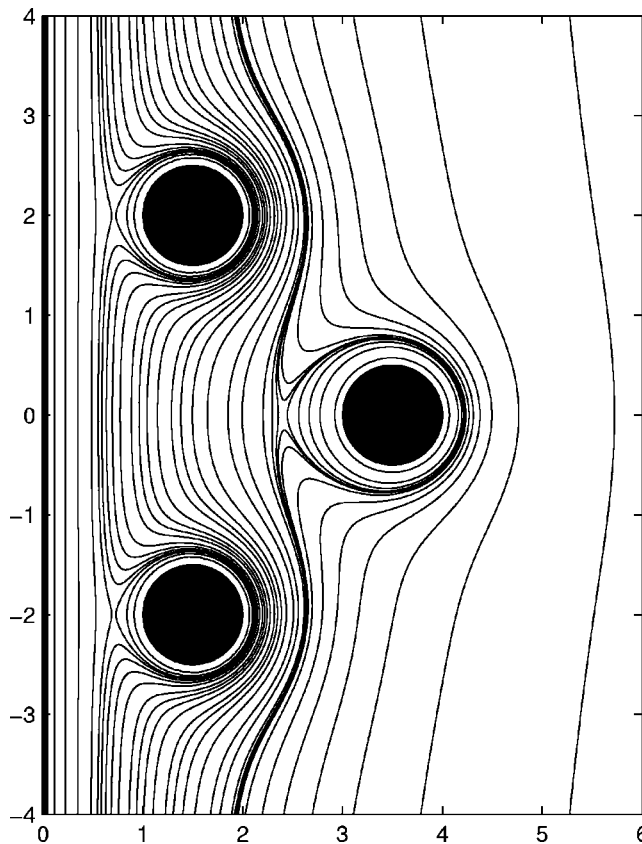


FIG. 13. Trajectories for three islands near a coastline. All have unit diameter, two are centered at  $1.5 \pm 2i$  and the other is centered at  $3.5$ .

complex) parameter  $b$  is chosen to appropriately locate its center. Clearly,  $\zeta=0$  maps to physical infinity so we have chosen  $\zeta_\infty=0$ . On use of (48) in (47), the Hamiltonian is

$$H^{(z)}(z_\alpha, \bar{z}_\alpha) = -\frac{\Gamma^2}{8\pi} \ln \left| \frac{\alpha^2 \omega'(\alpha, \alpha) \bar{\omega}'(\alpha^{-1}, \alpha^{-1}) \omega^2(\alpha, \infty) \bar{\omega}^2(\alpha^{-1}, 0)}{a^2 \omega(\alpha, \bar{\alpha}^{-1}) \bar{\omega}(\alpha^{-1}, \bar{\alpha}) \omega^2(\alpha, 0) \bar{\omega}^2(\alpha^{-1}, \infty)} \right|, \tag{49}$$

where the formulas in (46) must be used.

Again, let  $Q_j$  be the radius and  $D_j$  the position of the center of the  $j$ th circle ( $j=1, \dots, M$ ) in the physical plane. It remains to determine the parameters  $\{q_j, \delta_j | j=1, \dots, M\}$  from the known parameters  $a, b, \{Q_j, D_j | j=1, \dots, M\}$ . It is straightforward to show that the equations relating these parameters are given by

$$D_j = b + \frac{a \bar{\delta}_j}{|\delta_j|^2 - q_j^2} \tag{50}$$

and

$$Q_j = \frac{q_j |a|}{|\delta_j|^2 - q_j^2}. \tag{51}$$

Since  $\zeta=0$  maps to infinity, and therefore cannot be inside any of the circles  $\{C_j | j=1, \dots, M\}$ , then necessarily  $|\delta_j|^2 > q_j^2$  for all  $j=1, \dots, M$  so that  $Q_j > 0$  as required.

By way of examples, Figs. 15 and 16 show the cases of three and four unit-diameter islands equispaced (with unit separation) in an unbounded ocean. All vortex paths are closed and the critical trajectory separates vortex paths that encircle one or other of the islands from vortex paths that encircle all of the islands. Figure 17 shows the trajectories around a randomly chosen island configuration with no geometrical symmetries so that, again,  $\bar{\omega} \neq \omega$ . It is the same

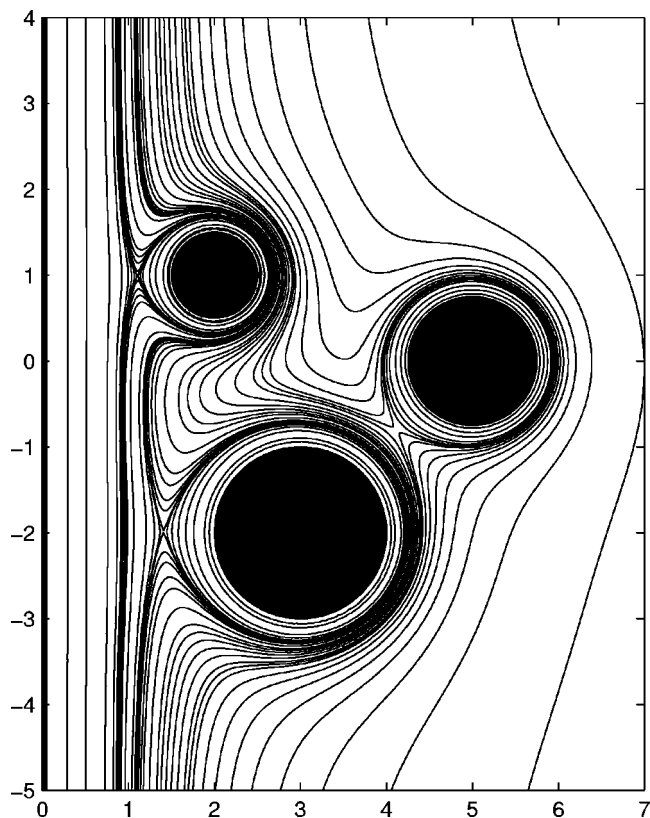


FIG. 14. Typical trajectories for vortices near three nonsymmetrically placed islands off a coastline. One island is centered at  $2+i$  with diameter 1, another is centered at  $3-2i$  with diameter 2, and a third centered at 5 with diameter 1.5.

island configuration as in Fig. 14 but with no coastline present.

In the case of unbounded oceans, more interesting vortex trajectories would be obtained if a background flow is incorporated. The effect of background flows requires the addition of another contribution (22) to the total Hamiltonian [see (21)]. However, finding a complex potential  $W_B(z)$  satisfying the no normal-flow boundary conditions on the islands even

for simple uniform or straining flows presents further mathematical challenges. Such extensions of the present work are currently under investigation.

### V. DISCUSSION

The formulas used in this paper, specifically, (20) and (47), are very general and are relevant to the flow of a single vortex in *any* multiply connected regions for which a conformal map  $z(\zeta)$  to the region from some multiply connected circular preimage region is known. Here, the two conformal maps (23) and (48) have been used to investigate various multi-island configurations in unbounded oceans and in oceans bounded by a coastline. It should be mentioned, however, that multiply connected circular preimage regions of the type exemplified in Fig. 1 are a standard set of canonical domains for general multiply connected conformal mappings.<sup>18</sup> Therefore, the formulas used in this paper are also those relevant to single-vortex motion in *arbitrary* multiply connected regions. If a mapping  $z(\zeta)$  to the domain of interest is known explicitly, then the Hamiltonian is also known explicitly on use of (20) or (47). If  $z(\zeta)$  is not known in analytical form, a numerical determination of such a map can nevertheless be used in the formulas above. The numerical determination of conformal maps is a standard procedure.<sup>20,21</sup> We also mention that while we have restricted attention here to the motion of a single vortex, the formulation presented in Crowdy and Marshall<sup>16</sup> extends to the general  $N$ -vortex problem.

A limitation of the formulas used in this paper is that the round-island circulations are zero. In certain physical situations, non-zero round-island circulations are relevant. We have not yet succeeded in generalizing the formulas of Ref. 16 to the general case of nonzero round-island circulations (although it turns out to be straightforward to do so in the special case of doubly connected domains). However, Lin<sup>6</sup> has demonstrated that this circumstance simply implies the addition of a further contribution to the total Hamiltonian—one that does not depend on the instantaneous point vortex positions. Lin refers to the contribution of nonzero round-

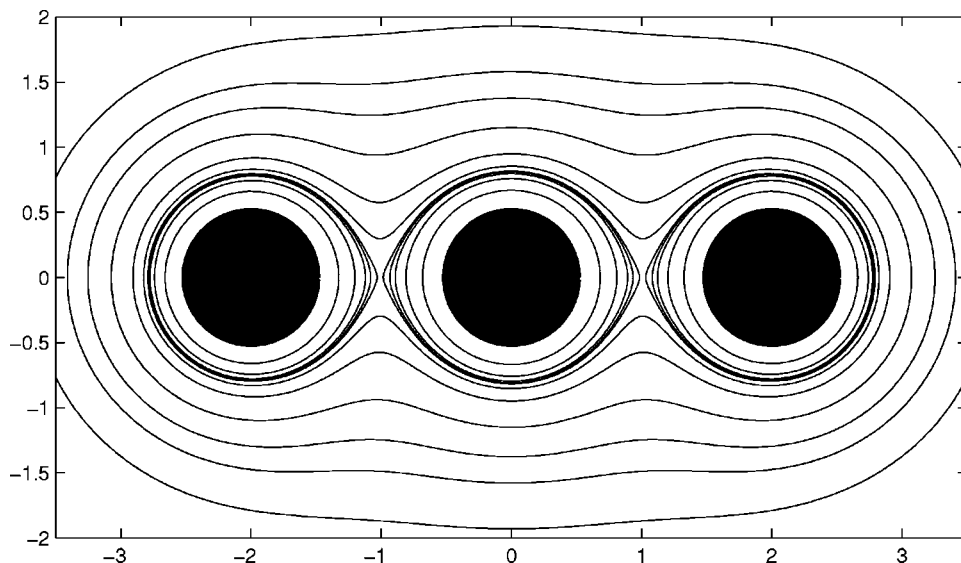


FIG. 15. Typical trajectories for three unit-diameter islands in an unbounded ocean and no background flow. The islands are separated by unit distance.

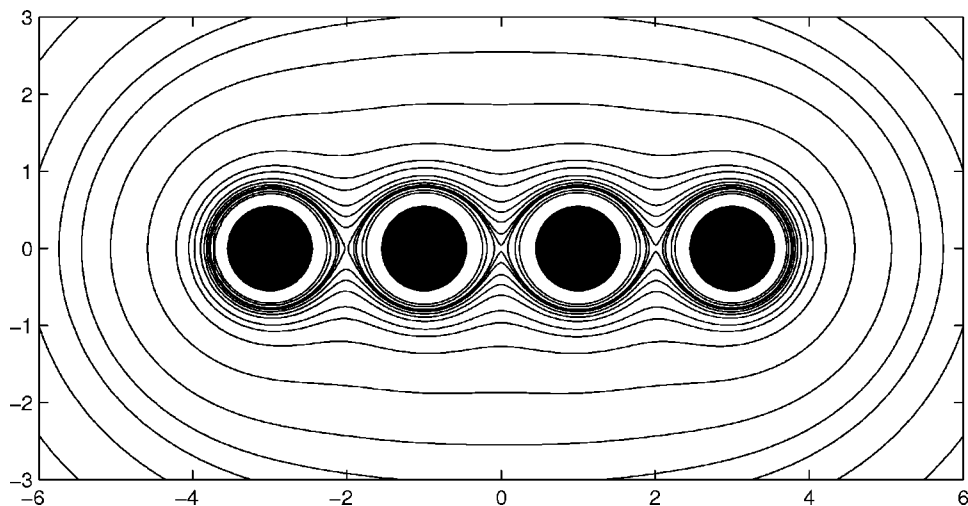


FIG. 16. Typical trajectories for four unit-diameter islands in an unbounded ocean and no background flow. The islands are separated by unit distance.

island circulations as being due to “external agencies” of vorticity (in general, these round-island circulations are fixed in time as a consequence of Kelvin’s circulation theorem). The fact that this additional Hamiltonian does not depend on the point vortex positions means that it can be determined (e.g., numerically, perhaps using boundary integral methods) at the start of any calculation and will remain fixed during the calculation if the contribution from the external agencies is time invariant. The explicit formulas of this paper can still be employed to give the “point vortex contribution” to the Hamiltonian. In this way, the formulas employed here should simplify the numerical computation of vortex trajectories even in the presence of nonzero round-island circulations.

The efficacy of our method has been demonstrated by a series of examples. It should be pointed out, however, that we have proceeded under the assumption that the infinite products defining the functions  $\omega$  and  $\bar{\omega}$  converge. In fact, these products do not converge for all choices of the parameters  $\{q_j, \delta_j | j=1, \dots, M\}$ —broadly speaking, their convergence depends on the distribution of circles  $\{C_j | j=1, \dots, M\}$  in the preimage plane. If the circles are “well separated” (in a sense that will be left imprecise here) then good convergence is assured. There is a large region of the parameter space  $\{q_j, \delta_j | j=1, \dots, M\}$  where the convergence is completely adequate for practical purposes, as we have demonstrated by example. This region of parameter space is large enough to capture all of the physically interesting fluid domains investigated herein.

This paper has made use of a general analytical framework in which to study the motion of a single vortex in general multiply connected flow domains. Given its generality, we expect the methodology to be useful in a variety of fluid dynamical contexts. We believe the power and usefulness of the method lies in the fact that it is algorithmically identical for flow regions of all finite connectivities.

## ACKNOWLEDGMENT

J.S.M. acknowledges the support of an EPSRC studentship.

<sup>1</sup>H. Aref, P. K. Newton, M. Stremler, T. Tokieda, and D. L. Vainchtein, “Vortex crystals,” *Adv. Appl. Mech.* **39**, 1 (2002).

<sup>2</sup>P. K. Newton, *The N-Vortex Problem* (Springer, New York, 2002).

<sup>3</sup>D. J. Acheson, *Elementary Fluid Dynamics* (Oxford University Press, Oxford, 1990).

<sup>4</sup>P. G. Saffman, *Vortex Dynamics* (Cambridge University Press, Cambridge, 1992).

<sup>5</sup>E. J. Routh, “Some applications of conjugate functions,” *Proc. R. Soc. London* **12**, 73 (1881).

<sup>6</sup>C. C. Lin, “On the motion of vortices in two dimensions—I. Existence of the Kirchhoff–Routh function,” *Proc. Natl. Acad. Sci. U.S.A.* **27**, 570 (1941).

<sup>7</sup>C. C. Lin, “On the motion of vortices in two dimensions—II. Some further investigations on the Kirchhoff–Routh function,” *Proc. Natl. Acad. Sci. U.S.A.* **27**, 575 (1941).

<sup>8</sup>M. Flucher and B. Gustafsson, “Vortex motion in two dimensional hydro-

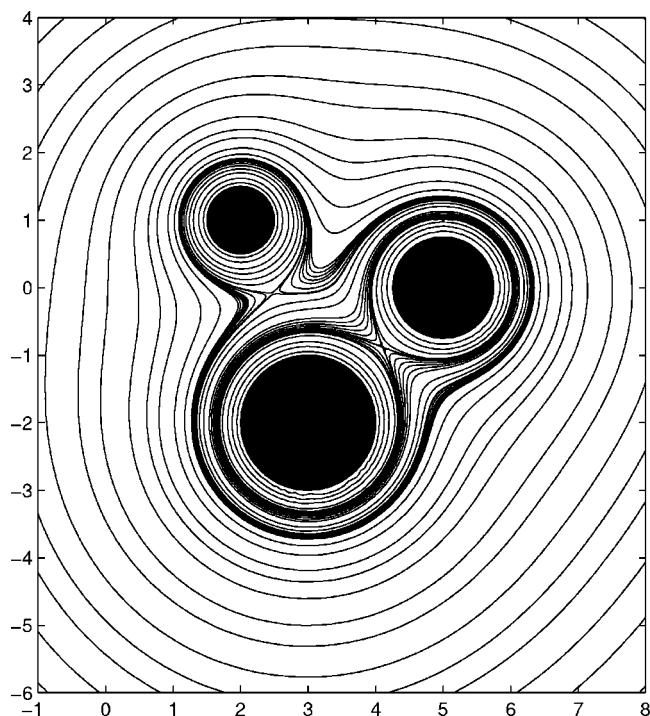


FIG. 17. Typical trajectories for three islands in an unbounded ocean and no background flow. The island configuration is the same as in Fig. 14 but there is now no coastline.

- dynamics,” Royal Institute of Technology Report No. TRITA-MAT-97-MA 02, 1997.
- <sup>9</sup>E. R. Johnson and N. R. McDonald, “The motion of a vortex near two circular cylinders,” *Proc. R. Soc. London, Ser. A* **460**, 939 (2004).
- <sup>10</sup>H. L. Simmons and D. Nof, “Islands as eddy splitters,” *J. Mar. Res.* **58**, 919 (2000).
- <sup>11</sup>W. K. Dewar, “Baroclinic eddy interaction with isolated topography,” *J. Phys. Oceanogr.* **32**, 2789 (2002).
- <sup>12</sup>H. L. Simmons and D. Nof, “The squeezing of eddies through gaps,” *J. Phys. Oceanogr.* **32**, 314 (2002).
- <sup>13</sup>D. Nof, “Choked flows from the Pacific to the Indian Ocean,” *J. Phys. Oceanogr.* **25**, 1369 (1995).
- <sup>14</sup>E. R. Johnson and N. R. McDonald, “The motion of a vortex near a gap in a wall,” *Phys. Fluids* **16**, 462 (2004).
- <sup>15</sup>R. Kidambi and P. Newton, “Vortex motion on a sphere with solid boundaries,” *Phys. Fluids* **12**, 581 (2000).
- <sup>16</sup>D. G. Crowdy and J. S. Marshall, “Analytical formulae for the Kirchhoff–Routh path function in multiply connected domains,” *Proc. R. Soc. London, Ser. A* (to be published).
- <sup>17</sup>M. J. Ablowitz and A. S. Fokas, *Complex Variables* (Cambridge University Press, Cambridge, 1997).
- <sup>18</sup>Z. Nehari, *Conformal Mapping* (McGraw-Hill, New York, 1952).
- <sup>19</sup>E. T. Whittaker and G. N. Watson, *A Course of Modern Analysis* (Cambridge University Press, Cambridge, 1927).
- <sup>20</sup>P. Henrici, *Applied and Computational Complex Analysis* (Wiley Interscience, New York, 1986).
- <sup>21</sup>T. K. DeLillo, M. A. Horn, and J. A. Pfaltzgraff, “Numerical conformal mapping of multiply connected regions by Fornberg-like methods,” *Numer. Math.* **83**, 205 (1999).